

## ORIGINAL ARTICLE

# Long noncoding RNA *TUG1* contributes to cerebral ischaemia/reperfusion injury by sponging mir-145 to up-regulate *AQP4* expression

Weifeng Shan<sup>1</sup> | Wei Chen<sup>2</sup>  | Xian Zhao<sup>1</sup> | Aijie Pei<sup>1</sup> | Manli Chen<sup>1</sup> | Yang Yu<sup>1</sup> | Yueying Zheng<sup>1</sup> | Shengmei Zhu<sup>1</sup> 

<sup>1</sup>Department of Anesthesiology, The 1st Affiliated Hospital, School of Medicine, Zhejiang University, Hangzhou, China

<sup>2</sup>Cancer Institute of Integrated traditional Chinese and Western Medicine, Zhejiang Academy of Traditional Chinese Medicine, Tongde hospital of Zhejiang Province, Hangzhou, China

## Correspondence

Shengmei Zhu and Yueying Zheng, Department of Anesthesiology, The 1st Affiliated Hospital, School of Medicine, Zhejiang University, 79# Qingchun Road, Hangzhou 310003, Zhejiang, China. Emails: 1185027@zju.edu.cn (SZ); 1507128@zju.edu.cn (YZ)

## Funding information

This work was supported by the National Natural Science Foundation of China (Grant No. 81471171, 81771194), Shengmei Zhu and by Zhejiang medical and health science and technology project (NO. 2016KYB106), Weifeng Shan

## Abstract

Emerging studies have shown that long noncoding RNA (lncRNA) *TUG1* (taurine-up-regulated gene 1) plays critical roles in multiple biological processes. However, the expression and function of lncRNA *TUG1* in cerebral ischaemia/reperfusion injury have not been reported yet. In this study, we found that lncRNA *TUG1* expression was significantly up-regulated in cultured MA-C cells exposed to OGD/R injury, while similar results were also observed in MCAO model. Mechanistically, knockdown of *TUG1* decreased lactate dehydrogenase levels and the ratio of apoptotic cells and promoted cell survival in vitro. Moreover, knockdown of *TUG1* decreased *AQP4* (encoding aquaporin 4) expression to attenuate OGD/R injury. *TUG1* could interact directly with miR-145, and down-regulation of miR-145 could efficiently reverse the function of *TUG1* siRNA on *AQP4* expression. Finally, the *TUG1* shRNA reduced the infarction area and cell apoptosis in I/R mouse brains in vivo. In summary, our results suggested that lncRNA *TUG1* may function as a competing endogenous RNA (ceRNA) for miR-145 to induce cell damage, possibly providing a new therapeutic target in cerebral ischaemia/reperfusion injury.

## KEYWORDS

Aquaporin-4, cerebral ischaemia, lncTUG1, miR-145, reperfusion injury

## 1 | INTRODUCTION

Ischaemia/reperfusion (I/R) is considered important for the recovery of ischaemic brain injury and also limits subsequent infarction development.<sup>1</sup> However, ischaemia/reperfusion induces apoptosis, inflammation and the overproduction of reactive oxygen species (ROS), thus leading to neuronal injury.<sup>2</sup> Thrombolytic therapy has been the only accepted treatment for cerebral I/R injury in clinics.<sup>2,3</sup> However, this therapy inevitably leads to ischaemia/reperfusion

injury (IRI) and its treatment effect is limited. Accumulating evidence shows that apoptosis and death of nerve cells after I/R are the main causes of aggravating brain injury.<sup>4,5</sup> Therefore, it is important to develop novel therapeutic strategies to treat cerebral IRI.

In the human genome, only 2% of the DNA is translated into proteins, suggesting that the majority of the genome remains either un-transcribed or (more often) transcribed into non-protein-coding RNAs.<sup>6</sup> According to their length, non-protein-coding RNAs are divided into two groups, small and long noncoding RNAs. Long

Shan and Chen contribute equally to this work.

This is an open access article under the terms of the Creative Commons Attribution License, which permits use, distribution and reproduction in any medium, provided the original work is properly cited.

© 2019 The Authors. Journal of Cellular and Molecular Medicine published by John Wiley & Sons Ltd and Foundation for Cellular and Molecular Medicine.

noncoding RNAs (lncRNAs) are longer than 200 nucleotides. They cannot be translated into proteins; therefore, initially, lncRNAs were considered as non-functional junk. However, currently, they are thought to participate in the regulation of protein expression.<sup>7,8</sup> Taurine-up-regulated gene 1 (*TUG1*), a 7.1-kb gene located at chr22q12.2, was initially identified as a transcript up-regulated in retinal cells treated with taurine.<sup>9</sup> Increasing evidence suggests that *TUG1* is involved in the development of a variety of cancers, including laryngeal squamous cell carcinoma and ovarian cancer.<sup>10,11</sup> It has been also reported that *TUG1* was up-regulated in the brain of middle cerebral artery occlusion (MCAO) and oxygen-glucose deprivation (OGD)-treated SH-SY5Y cells, indicating the therapeutic potential of *TUG1* in I/R.<sup>12</sup> However, there is limited knowledge on how *TUG1* acts at the molecular level and its exact role in I/R.

Recently, many studies have demonstrated that lncRNAs regulate gene expression at various levels, including chromatin modification, transcriptional regulation and post-transcriptional regulation.<sup>13</sup> lncRNAs can act as competing endogenous RNAs (ceRNAs) to reduce the concentrations of microRNAs (miRNAs), resulting in inhibition of miRNA functions in cells.<sup>14</sup> For example, lncRNA *TUG1* promotes cell proliferation and metastasis by negatively regulating miR-300 in gallbladder carcinoma.<sup>15</sup> In addition, *TUG1* alleviates extracellular matrix accumulation via mediating microRNA-377 targeting of PPAR in diabetic nephropathy.<sup>16</sup> These results prompted us to explore the mechanism of *TUG1* in cerebral I/R.

Aquaporin-4 (AQP4) is mainly expressed in astrocyte, particularly on the end of astrocyte at the blood-brain barrier.<sup>17</sup> Early study has shown that AQP4 inhibition in mice reduces brain oedema after ischaemic stroke.<sup>18</sup> Evidence has revealed that AQP4 is involved in enhancing brain oedema and AQP4 inhibition reduced brain oedema and infarct volume after ischaemic.<sup>19</sup> Our previous studies also showed that AQP4 overexpression could aggravate astrocyte ischaemic/reperfusion injury.<sup>20,21</sup>

In the present study, we employed a MCAO model and MA-C cell oxygen-glucose deprivation and reperfusion (OGD/R) model to determine whether *TUG1* expression was altered in cerebral IRI. We found that *TUG1* was significantly up-regulated after OGD/R treatment and in the MCAO model. Subsequent functional studies revealed that *TUG1* silencing attenuated the OGD/R injury both in vitro and in vivo. Mechanistically, *TUG1* acts as a miRNA sponge to positively modulate the expression of AQP4 by sponging miR-145. Therefore, our study provides new insights into the molecular function of the *TUG1*/miR-145/AQP4 signalling pathway in the pathogenesis of cerebral IRI and highlights the potential of lncRNAs to act as new therapeutic targets in cerebral IRI.

## 2 | MATERIALS AND METHODS

### 2.1 | Primary cultures of cerebellar astrocytes

Primary mouse astrocytes were obtained from a post-natal day (PND) 7 cerebral cortex, as previously described.<sup>22</sup> Briefly, brain

regions were dissected, mechanically dissociated and incubated with trypsin, followed by trituration, repeated washing and filtering. After counting, cells were plated at a density of  $10^7$  cells in 75 cm<sup>2</sup> tissue culture flasks pre-coated with poly-D-lysine and grown in Dulbecco's modified Eagle's medium (DMEM; Gibco) containing 10% fetal bovine serum (FBS), 100 U/mL penicillin and 100 µg/mL streptomycin at 37°C in 5% CO<sub>2</sub>.

### 2.2 | Establishment of the OGD/R model and MCAO model

To simulate an in vitro ischaemic-like condition, MA-C cells were subjected to OGD. The culture medium was replaced with deoxygenated glucose-free DMEM, and cells were incubated in a hypoxic chamber containing 5% CO<sub>2</sub>, 1% O<sub>2</sub> and 94% N<sub>2</sub> for 6 hours. Subsequently, the MA-C cells were returned to glucose-containing DMEM under normal culture conditions for 24 or 48 hours for reoxygenation. The overall protocol is known as OGD/R treatment.

C57/BL6 male mice were used in this study. All animal experiment protocols were approved by the animal committee at Zhejiang University. Healthy adult C57BL/6 mice were injected with intraperitoneal anaesthesia (4% chloral hydrate). The left common carotid artery, internal carotid artery and external carotid artery were separated sequentially from the left lateral approach to the neck. A silicone cord was inserted from the common carotid artery to the middle cerebral artery. After 60 minutes of embolization, the cord was removed and ligated.

Mice were randomly divided into four groups: (a) Sham: threading without occlusion, followed by persistent perfusion (n = 5); (b) I/R group: 1 hour of ischaemia and 24 hours of reperfusion (n = 5); (c) I/R + NC: mice were administrated with negative control shRNA (sh-NC; NC; 0.5 mg/kg, via intracerebroventricular injection) before ischaemia treatment (n = 5) and (d) I/R + *TUG1* shRNA: mice were administrated with *TUG1* shRNA (0.5 mg/kg, via intracerebroventricular injection) before ischaemic treatment (n = 5). *TUG1* shRNA or sh-NC was injected into the right cerebral ventricle of mice. One day post-injection, MCAO operation was established.

### 2.3 | Transfection of *TUG1* siRNA, miR-145 mimic, miR-145 inhibitor or AQP4 siRNA

To investigate the lncRNA *TUG1*'s function in OGD/R-treated MA-C cells, miR-145 mimics, inhibitors, negative control miRNA, *TUG1* siRNA, AQP4 siRNAs, or negative siRNA, or two of these treatments were transfected into cells at working concentrations [1:1 (v/v)] using Lipofectamine™ 2000 Transfection reagent (Invitrogen; Thermo Fisher Scientific, Inc) according to the manufacturer's protocol. After 6 hours of transfection, MA-C cells underwent OGD/R treatment (6-hour OGD and 24-hour reoxygenation). The transfection efficiencies of the miRNA or siRNA in MA-C cells were confirmed by quantitative real-time reverse-transcription polymerase chain reaction (qRT-PCR) to measure miR-145 or AQP4 expression. The

transfection efficiencies of the AQP4 siRNA were confirmed using Western blotting analysis.

## 2.4 | Real-time polymerase chain reaction

Total RNA was isolated from cultured primary astrocytes or ischaemic hemisphere from MCAO mice using the TRIzol reagent (Invitrogen) following the manufacturer's protocol, and the RNA concentration was measured spectrophotometrically. Single-stranded cDNA was synthesized using a cDNA synthesis kit (Takara) according to the manufacturer's procedures. RT-PCR assays were performed using Applied Biosystems SYBR Green Mix kits (Applied Biosystems). The following primers were used:

Tug1-FCAGTTCTTGCAACAGGTGAGC

Tug1-RTACTTCAGTAGGGCCAGCCA

AQP4-F GACAGACCCACAGCAAGG

AQP4-F GCAAAGGGAGATGAGAACC

mir-145 GTCCAGTTTCCCAGGAATCCCT

All experiments were repeated three times, and the results were normalized to the expression of actin or U6 mRNA.

## 2.5 | Western blot analysis

Proteins from cultured primary astrocytes were extracted using protein lysis solution (Cell Signaling Technology, Inc) containing protease inhibitors (Sigma-Aldrich; Merck KGaA) and centrifuged at  $12\,000 \times g$  for 5 minutes at 4°C. The supernatant was collected and quantified using the bicinchoninic acid method. Equivalent amounts of proteins (40 µg/lane) were separated on 10% SDS-PAGE gels and then transferred to polyvinylidene fluoride (PVDF) membranes (Millipore). The membranes were blocked with 5% non-fat milk in TBST buffer for 1 hour and then incubated overnight with the following primary antibodies: anti-AQP4 (ab46182, Abcam) and anti-β-actin (66009-1, Proteintech).

After being washed twice with TBST, the membranes were incubated with a horseradish peroxidase-conjugated secondary antibody, anti-rabbit-HRP (7074, Cell Signaling Technology [CST]) or anti-mouse-HRP (7076, CST) at 1:2000 dilution. Specific bands were visualized using an enhanced chemiluminescence detection kit.

## 2.6 | Lactate dehydrogenase assay

The death of MA-C cells was evaluated using a cytotoxicity lactate dehydrogenase (LDH) assay kit (DOJINDO) according to the manufacturer's protocol. Briefly, MA-C cells were cultured in 6-well plates, following OGD/R treatment and transfection. MA-C cells were collected, resuspended and cultured in 96-well plates in 37°C in CO<sub>2</sub> for the appropriate time. Then, 10 µL of Lysis Buffer was added and the cells were cultured at 37°C in CO<sub>2</sub> for 30 minutes. Working solution was then added at 100 µL per well, and the samples were

cultured at room temperature in the dark. Stop solution (50 µL) was then added to each well, and LDH levels in the culture supernatant were analysed immediately by measuring the absorbance at 490 nm using a microplate reader. LDH levels in the control group were expressed as 100%, and the levels in other groups were normalized to this value.

## 2.7 | Cell health assay

Live or dead MA-C cells were evaluated using a Calcein-AM/PI Double Stain Kit (DOJINDO) according to the manufacturer's protocol. Briefly, MA-C cells were cultured in 6-well plates, following OGD/R treatment and transfection. MA-C cells were collected, resuspended and cultured in 96-well plates in 37°C CO<sub>2</sub> for the appropriate time. Calcein-AM reserve solution (10 µL) and 15 µL of propidium iodide (PI) reserve solution were added to 5 mL of serum-free medium to prepare the dyeing solution. The final concentration of Calcein-AM was 2 µmol/L, and the final concentration of PI was 4 µmol/L. Dyeing solution (100 µL) was added each well. The cells were then cultured 37°C for 30 minutes before washing twice with phosphate-buffered saline (PBS). Live cells were detected by excitation at 490 nm, and dead cells were detected by excitation at 545 nm using a microplate reader.

## 2.8 | TdT-mediated biotin-16-dUTP nick-end labelling assay

The TdT-mediated biotin-16-dUTP nick-end labelling (TUNEL) assay was performed using a One-Step TUNEL Apoptosis Assay kit (Roche) to detect apoptotic cells in the mouse brain. In brief, 4-µm-thick paraffin sections were deparaffinized, hydrated, treated with proteinase K for 20 minutes and subsequently incubated with a mixture of a fluorescently labelled solution of dUTP and the TdT enzyme at 37°C for 1 hour in a humidified atmosphere. As a positive control, sections were incubated with DNase I for 10 minutes at room temperature (25°C) before the fluorescent labelling procedure. Negative controls were incubated with dUTP for 10 minutes at room temperature (25°C). Subsequently, the samples were treated with diaminobenzidine, counterstained with haematoxylin (to identify the cell nuclei). The cells were then dehydrated in a gradient ethanol series, vitrified with dimethylbenzene and mounted with neutral balsam.

## 2.9 | 2,3,5-Triphenyltetrazolium chloride measurement

Animals were anaesthetized with 4% chloral hydrate, and brain tissues were sectioned coronally and consecutively at 2-mm thick. Coronal brain slices were incubated in 1% 2,3,5-Triphenyltetrazolium chloride (TTC) buffer, at 37°C for 20 minutes. After incubation, the brain slices were fixed in 4% paraformaldehyde for 24 hours and then photographed. The red regions represented non-infarcted tissue regions, and pale white regions are infarcted tissue regions.

## 2.10 | Neurological function assessment

The severity of the injury of treated mice was assessed using a modified Bederson score as previously described.<sup>23</sup> The modified Bederson scores were as follows: 0, no deficit; mice with score 1, lost forelimb flexion; 2, as for 1, but plus decreased resistance to a lateral push; 3, indicated unidirectional circling; mice with score 4 displayed longitudinal spinning or seizure activity; mice with score 5 showed no movement.

## Luciferase reporter assay

293T cells were seeded in a 24-well plate. After 24 hours, miR-145-5p mimics or miR-NC was cotransfected with TUG1-wt (wild type) or TUG1-mut (mutant) into 293T cells using Lipofectamine 3000 (Invitrogen), dual-luciferase reporter assay system (Promega) were applied at 48 hours after transfection according to the manufacturer's instructions.

## 2.11 | Apoptosis assay

Apoptosis was detected using an Annexin V-FITC Apoptosis Detection Kit (DOJINDO) according to the manufacturer's protocol. Briefly, MA-C cells were cultured in 6-well plates, following OGD/R treatment and transfection. The cells were collected, resuspended with 195  $\mu$ L Annexin V-FITC binding solution. Annexin V-FITC (5  $\mu$ L) was then added, mixed gently and incubated for 10 minutes at room temperature (20-25°C) in the dark. The cells were centrifuged, resuspended in 190  $\mu$ L of Annexin V-FITC binding solution. Then, 10  $\mu$ L of PI solution was added, mixed well and placed in ice bath. Data were acquired using a BD FACSCalibur flow cytometer and analysed using BD Cell Quest software.

## 2.12 | Immunofluorescence

Immunofluorescence was used to identify astrocytes. Cells were washed with cold PBS, fixed in 4% paraformaldehyde for 15 minutes, blocked with 5% serum at 37°C for 60 minutes and incubated with a 1:300 dilution of anti-glial fibrillary acidic protein (GFAP) antibodies (#3670; CST) at 4°C overnight. After washing with PBS three times, the cells were incubated with a 1:100 dilution of a secondary antibody (#4409; CST) at 37°C for 2 hours. 2-(4-amidinophenyl)-1H-indole-6-carboxamide (DAPI; Sigma-Aldrich; Merck KGaA) was used for nuclear staining at 37°C for 2 minutes, and the cells were then washed three times with PBS and observed using an inverted fluorescence microscope (Olympus Corp.).

## 2.13 | Statistical analysis

Statistical analysis was performed using GraphPad Prism 5.0 software (GraphPad Software). Data were presented as a mean  $\pm$  standard deviation (SD). To compare the difference between two groups or multiple groups, a t test and one-way analysis of variance (ANOVA)

were performed, respectively. A difference was considered significant at  $P < .05$ .

## 3 | RESULTS

### 3.1 | TUG1 is highly expressed after OGD/R treatment

To investigate whether TUG1 expression was altered in cerebral IRI, TUG1 expression in MA-C cells was measured immediately following 6 hours of OGD and during different reoxygenation times using qRT-PCR. The morphological changes of MA-C cells under control or OGD/RX condition were shown in Figure S1. High levels of TUG1 were detected in the MCAO model (ischaemia for 1 hour and during different reperfusion time periods) compared with that in the control group ( $P < .05$ ; Figure 1A). Moreover, TUG1 levels were significantly up-regulated under OGD/R conditions compared with that under the control conditions ( $P < .05$ ; Figure 1B). These results suggested that the up-regulation of lncRNA TUG1 contributes to cerebral ischaemia injury.

Given that TUG1 is overexpressed in MA-C cells exposed to OGD/R treatment, we performed knockdown of TUG1 in vitro to investigate whether TUG1 plays a role in IRI. Three small interfering RNA (siRNAs) targeting the coding region of TUG1 (siTUG1-3) were tested for their knockdown efficiency. Cells were transfected with siTUG1-1, siTUG1-2, siTUG1-3 or a negative control. The efficiency of interference was verified by qRT-PCR (Figure S1). The effects of TUG1 on OGD/R were evaluated using LDH assays and cell health assays. Silencing of TUG1 significantly suppressed LDH leakage and promoted cell survival compared with the non-transfected OGD/R-treated group (Figure 1C-D). In addition, OGD/R treatment increased cell apoptosis while silencing of TUG1 prevented OGD/R-induced apoptosis (Figure 1E). These results suggested that OGD/R induces cell injury by up-regulating TUG1 expression.

### 3.2 | Knockdown of TUG1 attenuates the OGD/R injury by inhibiting the expression of AQP4

Our team has been studying AQP4 and brain tissue injury in the early stage and found that AQP4 plays an important role in cerebral injury in stroke.<sup>20,21</sup> This was confirmed in Figure S, which showed that knockdown of AQP4 inhibits cell apoptosis and LDH leakage, and increases cell health in OGD/R-treated MA-C cells. Therefore, we hypothesized that TUG1 might exert its function by regulating AQP4 expression. To confirm whether TUG1 regulates AQP4, MA-C cells were transfected with siTUG1-1, siTUG1-2, siTUG1-3 or the negative control. As expected, knockdown of TUG1 expression significantly decreased the accumulation of AQP4 (Figure 2A). Next, to confirm whether AQP4 mediates the damage of caused by TUG1 to MA-C cells exposed to OGD/RX, the cells were transfected with siAQP4, exposed to OGD/R, and then transfected with control, siTUG1-1, siTUG1-2 and siTUG1-3, respectively. OGD/R

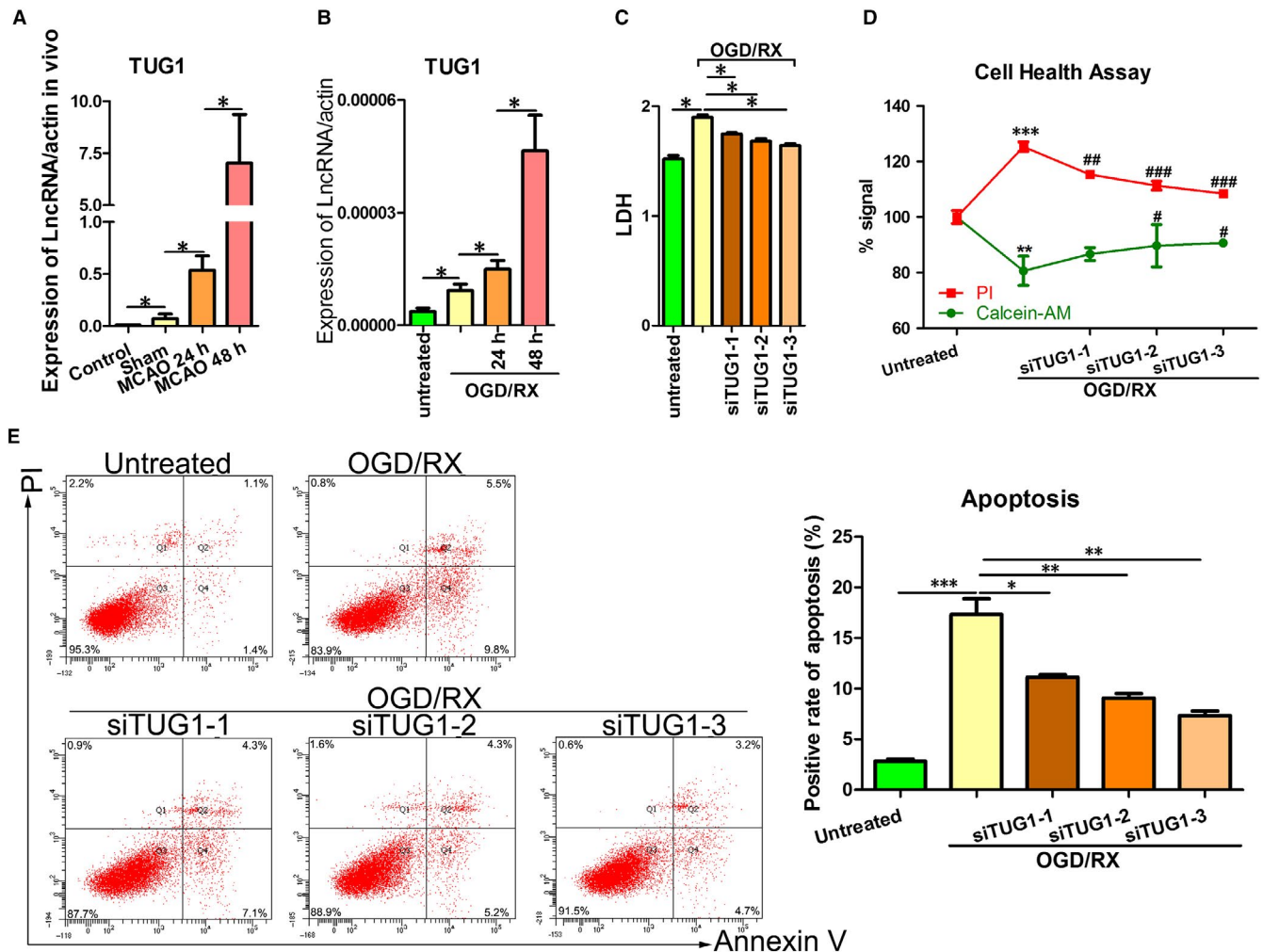


**FIGURE 1** *TUG1* was up-regulated in MA-C cells cultured under OGD/R conditions. A, QRT-PCR showing *TUG1* levels in MA-C cells at 24 or 48 h post-reoxygenation. B, *TUG1* levels were measured using qRT-PCR at 24 h/48 h post-reperfusion after MCAO was established. C, LDH leakage was measured using LDH assays after *TUG1* knockdown under OGD-R conditions (6-h OGD and 24-h reoxygenation). D, Cell health was measured using cell health assays after *TUG1* knockdown under OGD-R conditions (6-h OGD and 24-h reoxygenation). E, Flow cytometry assays were performed to show the cell apoptosis after transfection with short interfering RNAs siTUG1-1, siTUG1-2 and siTUG1-3 after 6-h OGD/24-h reoxygenation treatments. MCAO, middle carotid artery occlusion; OGD/R, oxygen-glucose deprivation and reperfusion; qRT-PCR, quantitative real-time reverse-transcription polymerase chain reaction; *TUG1*, taurine-up-regulated gene 1

treatment enhanced LDH leakage and suppressed cell viability, whereas knockdown of *AQP4* significantly attenuated the OGD/R treatment-induced damage. However, knockdown of *TUG1* did not further mitigate the damage (Figure 2B). The efficiency of siAQP4 interference was verified by qRT-PCR (Figure S1). In addition, after transfection with siAQP4, knockdown of *TUG1* did not further decrease the OGD/R treatment-induced apoptosis (Figure 2C). These results indicated that *TUG1* plays a role in cerebral IRI by regulating *AQP4* expression.

### 3.3 | *TUG1* directly interacts with miR-145 to regulate *AQP4* protein expression

Bioinformatic analysis of miRNA recognition sequences in *TUG1* was performed using miRcode. MiR-145 was identified as being capable of binding to complementary sequences in *TUG1* (Figure 3A). To

prove the prediction, we performed luciferase reporter assay. The results showed that *TUG1*-WT could significantly lower the luciferase activity in miR-145-5p group but had no significant effect on the luciferase activity of the miR-NC group (Figure 3B). To determine whether the expression of miR-145 is regulated by *TUG1*, we transfected MA-C cells with siTUG1-1, siTUG1-2 and siTUG1-3. After knockdown of *TUG1*, the miR-145 level was significantly up-regulated, indicating that *TUG1* negatively regulates miR-145 (Figure 3C).

To investigate the regulatory effect of miR-145 on *AQP4* expression, MA-C cells were transfected with a miR-145 mimic or miR-145 inhibitor. The miR-145 mimic decreased *AQP4* levels, while the miR-145 inhibitor increased *AQP4* levels (Figure 3D). OGD/R treatment significantly enhanced *AQP4* expression, while the miR-145 mimic significantly suppressed the *AQP4* expression induced by OGD/R treatment (Figure 3E). Taken together, these data indicated that knockdown of *TUG1* increased the expression of miR145 and

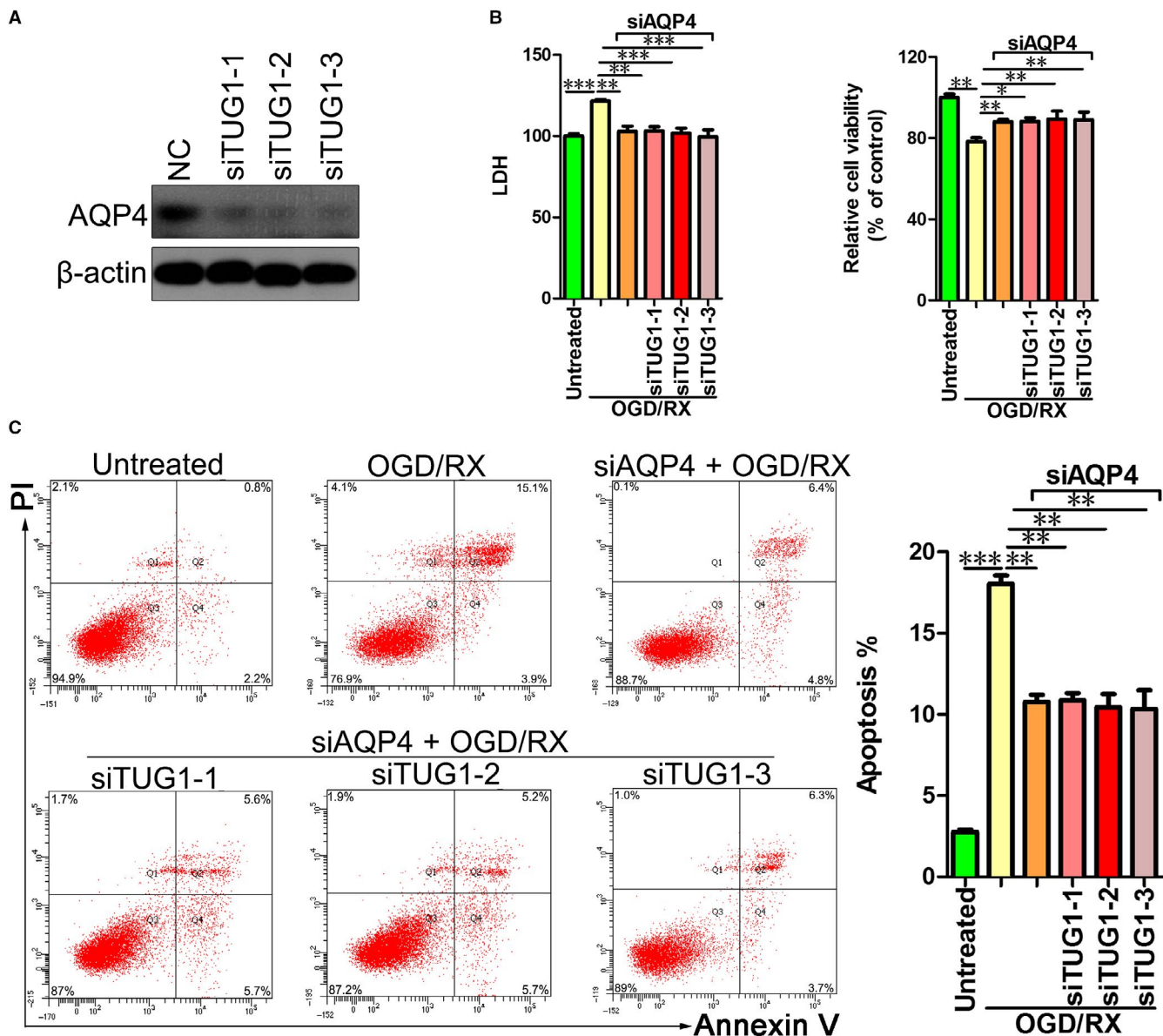


**FIGURE 2** Knockdown of *TUG1* attenuates the OGD/R injury by inhibiting the expression of AQP4. A, AQP4 protein levels in MA-C cells transfected with short interfering RNAs siTUG1-1, siTUG1-2 and siTUG1-3 as assessed using by Western blotting assays. B, LDH leakage (left) and cell viability were measured using LDH and CCK8 assays, respectively. MA-C cells were transfected with siTUG1-1, siTUG1-2 and siTUG1-3 in 6-h OGD/24-h reoxygenation treatments. C, Flow cytometry assays were performed to show the cell apoptosis after cotransfection with AQP4 siRNA and siTUG1-1, siTUG1-2 and siTUG1-3 in 6-h OGD/24-h reoxygenation treatments. AQP4, aquaporin 4; OGD/R, oxygen-glucose deprivation and reperfusion; siRNA, short interfering RNA; TUG1, taurine-up-regulated gene 1

inhibited the expression of AQP4 in MA-C cells exposed to OGD/R treatment.

### 3.4 | Mir-145 inhibitor reverses the protective effect of *TUG1* siRNA against OGD/R-induced injury in vitro

Considering the inhibitory action of *TUG1* on miR-145 levels in MA-C cells, we further explored the role of miR-145 in the protective effects of the *TUG1* siRNA against OGD/R-induced injury. Astrocytes were pretreated with the miR-145 inhibitor, transfected with untreated and

siTUG1-1, siTUG1-2 or siTUG1-3, and then exposed to OGD/R. LDH, cell health assays and cell apoptosis assays were performed. OGD/R treatment increased LDH leakage and decreased cell health, indicating that OGD/R treatment induces cell damage. Transfection of the miR-145 inhibitor further aggravated cell damage, while cotransfection of miR-145 inhibitor + si-TUG1 did not abolished the effects induced by the miR-145 inhibitor (Figure 4A-B). The efficiency of miR-145 inhibitor transfection was verified by qRT-PCR (Figure S1). In line with cell apoptosis, OGD/R treatment increased cell apoptosis compared with that in the untreated group. Transfection of the miR-145 inhibitor further enhanced cell apoptosis, while cotransfection of miR-145

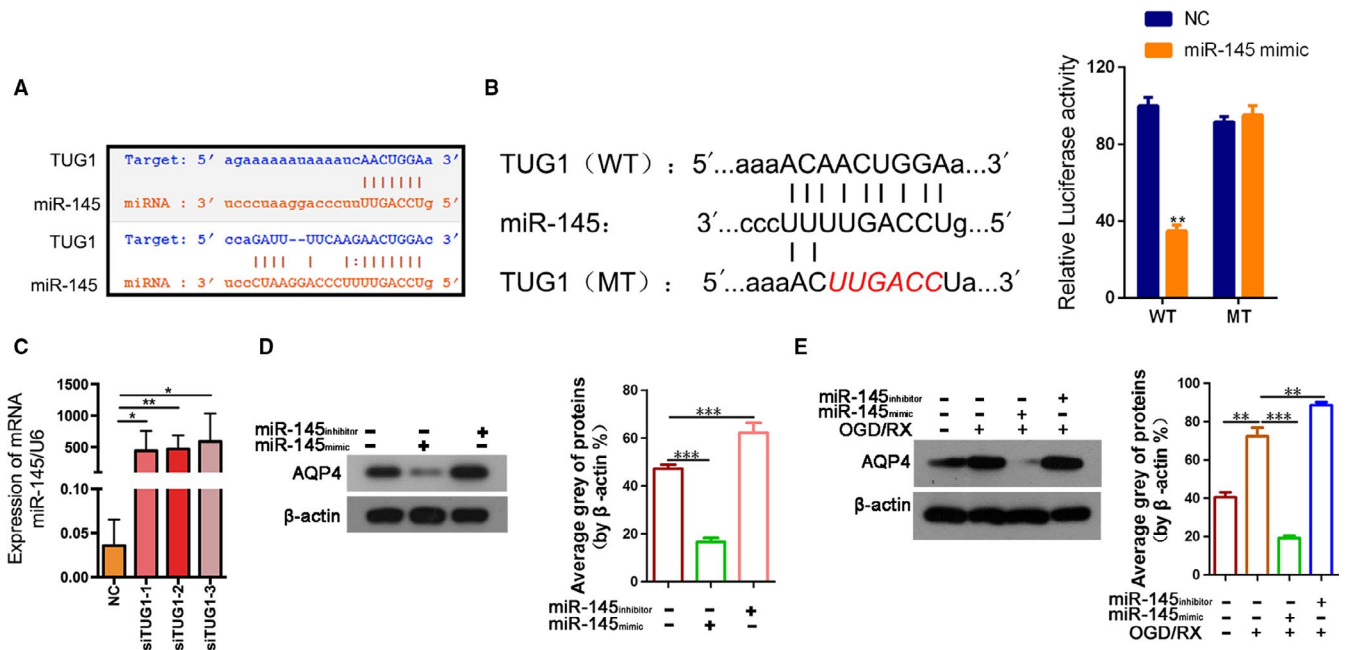


**FIGURE 3** *TUG1* directly targeted miR-145 and miR-145 regulates the expression of AQP4. A, Sequence alignment of predicted miR-145-binding sites within the *TUG1*. B, Schematic diagram showed the putative miR-145-5p-binding sites within the *TUG1*. The sequences of wild-type *TUG1* and mutant *TUG1* were listed as well. Luciferase reporter gene assays were performed to measure the luciferase activity in 293T cells.  $**P < .01$ . C, QRT-PCR assays were performed to analyse the expression level of miR-145 after transfection with siTUG1-1, siTUG1-2 and siTUG1-3. D, AQP4 protein level after transfection with miR-145 mimic or inhibitor was measured by Western blotting and quantified. E, AQP4 protein level after transfection with miR-145 mimic or inhibitor was measured in 6-h OGD/24-h reoxygenation treatments by Western blotting and quantified. AQP4, aquaporin 4; qRT-PCR, quantitative real-time reverse-transcription polymerase chain reaction; *TUG1*, taurine-up-regulated gene 1

inhibitor + si-*TUG1* did not decrease cell apoptosis, suggesting that the protective effect of *TUG1* siRNA had disappeared (Figure 4C-D).

Next, siTUG1-1 was chosen for further experiments. Astrocytes were pretreated with siTUG1-1, transfected separately with untreated and miR-145 inhibitor, and then exposed to OGD/R. *TUG1* knockdown significantly reduced LDH leakage, whereas cotransfection of the miR-145 inhibitor + si-*TUG1* did not reduce LDH leakage (Figure 4E). In addition, apoptosis assays showed that *TUG1* knockdown significantly decreased cell apoptosis under OGD/R treatment, while cotransfection of the miR-145 inhibitor + si-*TUG1* did not decrease cell apoptosis (Figure 4F-G). Collectively, these results demonstrated the *TUG1* siRNA protects against cerebral IRI by up-regulating miR-145 levels.

### 3.5 | In vivo, *TUG1* shRNA reduces the infarction area and cell apoptosis in I/R mice brains

To demonstrate the protective role of *TUG1* against brain I/R injury, we first established the MCAO model in mice and determined the effect of *TUG1* on infarction area using TTC staining, with Sham, MCAO, MCAO + NC and MCAO + *TUG1* shRNA groups. As shown in Figure 5A, the infarct region was observed in the brain of both MCAO and MCAO + NC groups. However, the infarct area was significantly reduced in the MCAO group + *TUG1* shRNA group (Figure 5B). Meanwhile, we used the Bederson score to rate the functional neurological deficits in MCAO mice after transfection

with or without *TUG1* shRNA. The results showed that the Bederson score decreased significantly after *TUG1* knockdown (Figure 5C). Moreover, TUNEL analysis revealed that *TUG1* knockdown could significantly decrease the rate of apoptosis in MCAO mice (Figure 5D). Our data indicated that *TUG1* knockdown effectively protects against brain tissue damage in MCAO model mice.

## 4 | DISCUSSION

Although evidence has demonstrated the ectopic expression of lncRNA *TUG1* in many cancers,<sup>10,11,24</sup> its expression and biological role in cerebral IRI remain uncharacterized. Our study confirmed that *TUG1* expression was significantly higher after OGD/R treatment compared with that in the control group. High *TUG1* expression was also found in MCAO model mice compared with the control group. Moreover, shRNA-mediated silencing of *TUG1* reduced the infarction area and cell apoptosis in I/R mouse brains. Together, these data support the concept that *TUG1* is associated with cerebral IRI and functions as a positive regulator in IRI progression. A new mechanism has been proposed in which lncRNA *H19* induces cerebral ischaemia-reperfusion injury<sup>25</sup> and more recently, Weixin et al.<sup>5</sup> demonstrated that lncRNA *MALAT1* inhibits apoptosis induced by oxygen-glucose deprivation and reoxygenation in human brain microvascular endothelial cells. From these studies, a broader understanding of the mechanisms of action of more

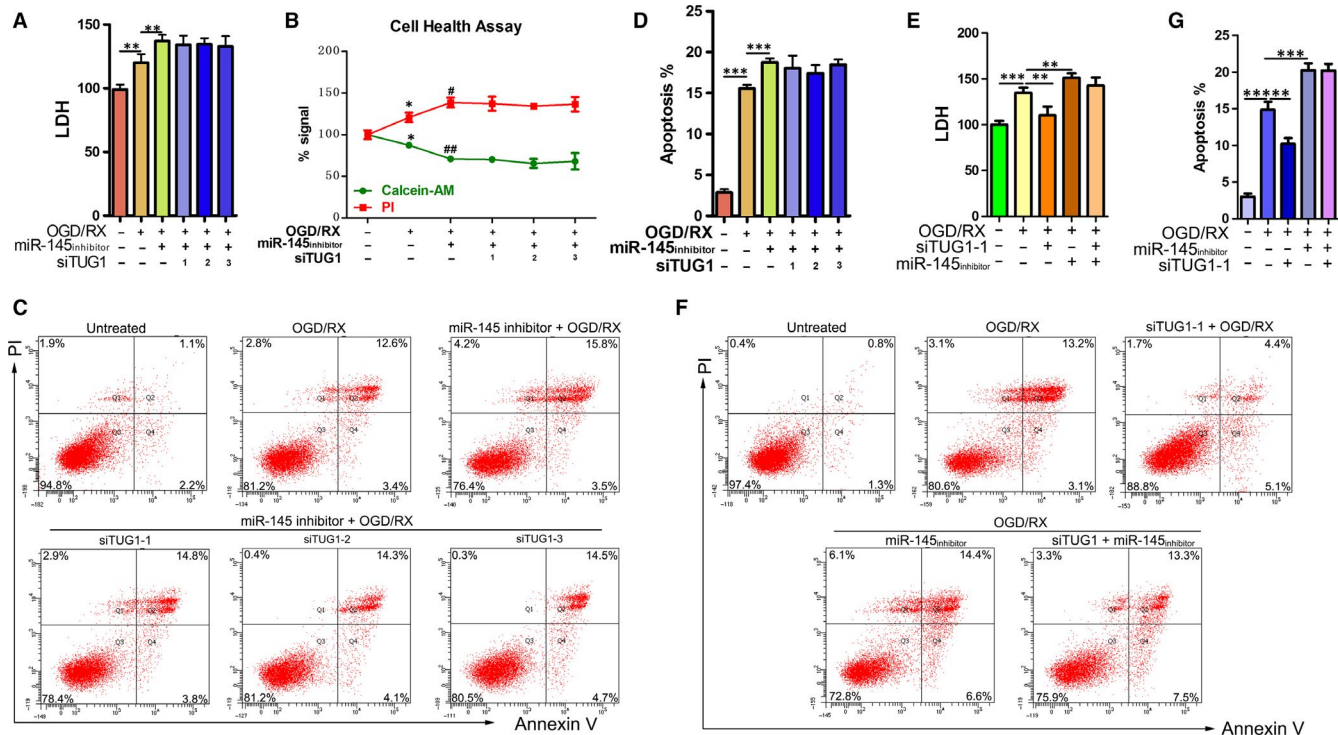


**FIGURE 4** Changes in cell damage in OGD/R-treated MA-C cells cotransfected with the miR-145 inhibitor and siTUG1. A, LDH leakage and B, cell health were measured using LDH assays and cell health assays. MA-C cells were cotransfected with mir-145 inhibitor and siTUG1-1, siTUG1-2 or siTUG1-3 in 6-h OGD/24-h reoxygenation treatments. C-D, Flow cytometry assays were performed to show the cell apoptosis after cotransfection with mir-145 inhibitor and siTUG1-1, siTUG1-2 or siTUG1-3 in 6-h OGD/24-h reoxygenation treatments. E, LDH leakage was measured using LDH assays after cotransfection with mir-145 inhibitor and siTUG1-1 in 6-h OGD/24-h reoxygenation treatments. F-G, Flow cytometry assays were performed to show the cell apoptosis after cotransfection with mir-145 inhibitor and siTUG1-1 in 6-h OGD/24-h reoxygenation treatments. OGD/R, oxygen-glucose deprivation and reperfusion; TUG1, taurine-up-regulated gene 1

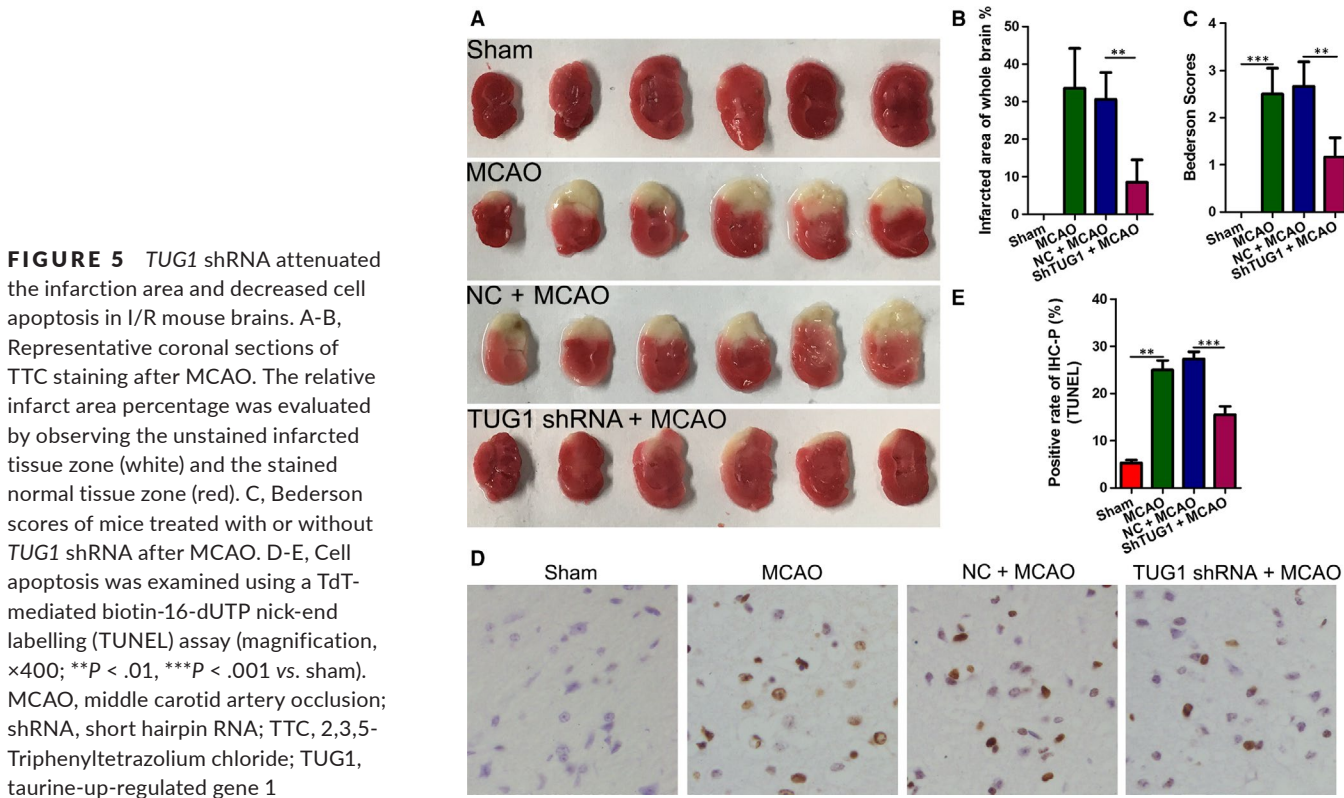


**FIGURE 5** TUG1 shRNA attenuated the infarction area and decreased cell apoptosis in I/R mouse brains. A-B, Representative coronal sections of TTC staining after MCAO. The relative infarct area percentage was evaluated by observing the unstained infarcted tissue zone (white) and the stained normal tissue zone (red). C, Bederson scores of mice treated with or without TUG1 shRNA after MCAO. D-E, Cell apoptosis was examined using a TdT-mediated biotin-16-dUTP nick-end labelling (TUNEL) assay (magnification,  $\times 400$ ;  $^{**}P < .01$ ,  $^{***}P < .001$  vs. sham). MCAO, middle carotid artery occlusion; shRNA, short hairpin RNA; TTC, 2,3,5-Triphenyltetrazolium chloride; TUG1, taurine-up-regulated gene 1



lncRNAs may further the development of new therapeutic strategies for cerebral IRI.

Aquaporin-4 (AQP4), a member of the water channel family, is mainly expressed in astrocytes, ependymal cells, soft meninges, choroid plexus and the nucleus of the lower mound in the brain.<sup>17,26</sup> Increasing evidence indicates that AQP4 plays an important role in cerebral ischaemia/reperfusion. Combination therapy of Emodin and GRb1 had a neuroprotective effect via the down-regulation of AQP4 in cerebral ischaemia/reperfusion rats.<sup>27</sup> AQP4-null mice are protected from cellular (cytotoxic) brain oedema produced by water intoxication, brain ischaemia or meningitis.<sup>28</sup> Our previous studies showed AQP4 plays a role in cerebral ischaemic injury.<sup>20,21</sup> MiR-29a ameliorated ischaemic injury of astrocytes in vitro by targeting AQP4,<sup>20</sup> and up-regulation of miR-130b protects against cerebral ischaemic injury also by targeting AQP4.<sup>21</sup> Therefore, we hypothesized that *TUG1* exerts its function by regulating AQP4. First, knockdown of *TUG1* decreased the accumulation of the AQP4 protein. Second, *AQP4* silencing alleviated cellular damage. However, knockdown of *TUG1* did not further mitigate the damage. Third, after transfection with siAQP4, knockdown of *TUG1* did not further decrease the OGD/R treatment-induced apoptosis. The above data not only supported a pro-apoptosis role of AQP4 in cerebral ischaemic injury progression, but also revealed a novel mechanism by which an lncRNA induces cell damage by regulating AQP4 expression.

The mechanisms of action of lncRNAs include both transcriptional and post-transcriptional regulation. Recently, a new regulatory mechanism in which lncRNAs acting as ceRNAs to sponge miRNAs, thus participating in post-transcriptional processing, has been identified.<sup>29</sup> The miRNA sponge function of *TUG1* was supported by the evidence generated in the present study. First, we predicted the interaction between *TUG1* and miR-145 using bioinformatic analysis and found that *TUG1* indeed contains a target site of miR-145. Second, after knockdown of *TUG1*, the miR-145 level was significantly up-regulated, indicating that *TUG1* negatively regulates miR-145. Third, down-regulation of miR-145 level efficiently reversed the protective effect induced by the *TUG1* siRNA. These results confirmed that *TUG1* induces cell damage by regulating miR-145.

After confirming the positive relationship between *TUG1* and AQP4, as well as the negative correlation between *TUG1* and miR-145 during cerebral I/R injury, we also identified the downstream target of miR-145 in this mechanism. Overexpression of miR-145 via the miR-145 mimic decreased AQP4 accumulation, whereas down-regulation of miR-145 via the miR-145 inhibitor increased AQP4 levels. In addition, the miR-145 mimic reversed the AQP4 expression in the presence of OGD/R. These analyses showed that *TUG1* sponges miR-145 to induce cell damage by up-regulating AQP4. In fact, previous studies have shown that individual protein-coding genes can be regulated by multiple non-protein-coding RNAs, while one non-protein-coding RNA can regulate multiple protein-coding genes.<sup>30,31</sup> Thus, whether AQP4 could be regulated by other sponging lncRNAs, and whether *TUG1* could function as a sponge lncRNA to affect expressions of other key regulators in cerebral IRI, requires further investigation.

## 5 | CONCLUSION

In the present study, we identified *TUG1* as a novel positive regulator in the pathogenesis of cerebral IRI. Moreover, our findings shed light on the interaction between *TUG1* and miR-145 in IRI, and revealed that *TUG1* positively regulates post-transcriptional expression of AQP4 by sponging miR-145 in cerebral IRI. Knockdown of *TUG1* via siRNA decreased AQP4 expression, providing a novel therapeutic target for cerebral IRI.

## COMPETING INTERESTS

The authors declare that they have no competing interests.

## AUTHORS CONTRIBUTIONS

ZSM and ZYY conceived the research idea; SWF and CW performed the experiments; PAJ, CML and YY analysed the data; ZX wrote the manuscript. All authors read and approved the final version of the manuscript.

## ETHICAL APPROVAL AND CONSENT TO PARTICIPATE

All animal experiments were approved by the First Affiliated Zhejiang Hospital, Zhejiang University of Medical Ethics Committee, the Medical Faculty Ethics Committee of the First Affiliated Zhejiang Hospital, Zhejiang University in accordance with the National Institutes of Health Guide for Care and Use of Laboratory Animals (NIH Publications, No. 8023, revised 1978).

## ORCID

Wei Chen  <https://orcid.org/0000-0002-0399-6216>

Shengmei Zhu  <https://orcid.org/0000-0001-9763-4015>

## DATA AVAILABILITY STATEMENT

All data generated or analysed during this study are included in this published article.

## REFERENCES

- Huang Z, Lu L, Jiang T, et al. miR-29b affects neurocyte apoptosis by targeting MCL-1 during cerebral ischemia/reperfusion injury. *Exp Ther Med*. 2018;16:3399-3404.
- Duan Q, Sun W, Yuan H, Mu X. MicroRNA-135b-5p prevents oxygen-glucose deprivation and reoxygenation-induced neuronal injury through regulation of the GSK-3beta/Nrf2/ARE signaling pathway. *Arch Med Sci*. 2018;14:735-744.
- Wang SH, Ma F, Tang ZH, et al. Long non-coding RNA H19 regulates FOXM1 expression by competitively binding endogenous miR-342-3p in gallbladder cancer. *J Exp Clin Cancer Res*. 2016;35:160.

4. Cao L, Zhang Y, Zhang S, et al. MicroRNA-29b alleviates oxygen and glucose deprivation/reperfusion-induced injury via inhibition of the p53-dependent apoptosis pathway in N2a neuroblastoma cells. *Exp Ther Med*. 2018;15:67-74.
5. Xin JW, Jiang YG. Long noncoding RNA MALAT1 inhibits apoptosis induced by oxygen-glucose deprivation and reoxygenation in human brain microvascular endothelial cells. *Exp Ther Med*. 2017;13:1225-1234.
6. ENCODE Project Consortium. An integrated encyclopedia of DNA elements in the human genome. *Nature*. 2012;489:57-74.
7. Zhan Y, Zang H, Feng J, Lu J, Chen L, Fan S. Long non-coding RNAs associated with non-small cell lung cancer. *Oncotarget*. 2017;8:69174-69184.
8. Mercer TR, Mattick JS. Structure and function of long noncoding RNAs in epigenetic regulation. *Nat Struct Mol Biol*. 2013;20:300-307.
9. Young TL, Matsuda T, Cepko CL. The noncoding RNA taurine up-regulated gene 1 is required for differentiation of the murine retina. *Curr Biol*. 2005;15:501-512.
10. Liu S, Liu Y, Lu Q, Zhou X, Chen L, Liang W. The lncRNA TUG1 promotes epithelial ovarian cancer cell proliferation and invasion via the WNT/beta-catenin pathway. *Onco Targets Ther*. 2018;11:6845-6851.
11. Zhang Z, Wang X, Cao S, et al. The long noncoding RNA TUG1 promotes laryngeal cancer proliferation and migration. *Cell Physiol Biochem*. 2018;49:2511-2520.
12. Chen S, Wang M, Yang H, et al. LncRNA TUG1 sponges microRNA-9 to promote neurons apoptosis by up-regulated Bcl2l11 under ischemia. *Biochem Biophys Res Comm*. 2017;485:167-173.
13. Mercer TR, Dinger ME, Mattick JS. Long non-coding RNAs: insights into functions. *Nat Rev Genet*. 2009;10:155-159.
14. Ebert MS, Neilson JR, Sharp PA. MicroRNA sponges: competitive inhibitors of small RNAs in mammalian cells. *Nat Methods*. 2007;4:721-726.
15. Ma F, Wang SH, Cai Q, et al. Long non-coding RNA TUG1 promotes cell proliferation and metastasis by negatively regulating miR-300 in gallbladder carcinoma. *Biomed Pharmacother*. 2017;88:863-869.
16. Duan LJ, Ding M, Hou LJ, Cui YT, Li CJ, Yu DM. Long noncoding RNA TUG1 alleviates extracellular matrix accumulation via mediating microRNA-377 targeting of PPARgamma in diabetic nephropathy. *Biochem Biophys Res Comm*. 2017;484:598-604.
17. Papadopoulos MC, Verkman AS. Aquaporin water channels in the nervous system. *Nat Rev Neurosci*. 2013;14:265-277.
18. Manley GT, Fujimura M, Ma T, et al. Aquaporin-4 deletion in mice reduces brain edema after acute water intoxication and ischemic stroke. *Nat Med*. 2000;6:159-163.
19. Yao X, Derugin N, Manley GT, Verkman AS. Reduced brain edema and infarct volume in aquaporin-4 deficient mice after transient focal cerebral ischemia. *Neurosci Lett*. 2015;584:368-372.
20. Zheng Y, Pan C, Chen M, Pei A, Xie L, Zhu S. miR29a ameliorates ischemic injury of astrocytes in vitro by targeting the water channel protein aquaporin 4. *Oncol Rep*. 2019;41(3):1707-1717.
21. Zheng Y, Wang L, Chen M, Pei A, Xie L, Zhu S. Upregulation of miR-130b protects against cerebral ischemic injury by targeting water channel protein aquaporin 4 (AQP4). *Am J Transl Res*. 2017;9:3452-3461.
22. Guizzetti M, Costa P, Peters J, Costa LG. Acetylcholine as a mitogen: muscarinic receptor-mediated proliferation of rat astrocytes and human astrocytoma cells. *Eur J Pharmacol*. 1996;297:265-273.
23. Bederson JB, Pitts LH, Tsuji M, Nishimura MC, Davis RL, Bartkowski H. Rat middle cerebral artery occlusion: evaluation of the model and development of a neurologic examination. *Stroke*. 1986;17:472-476.
24. Li T, Chen Y, Zhang J, Liu S. LncRNA TUG1 promotes cells proliferation and inhibits cells apoptosis through regulating AURKA in epithelial ovarian cancer cells. *Medicine*. 2018;97:e12131.
25. Wang J, Cao B, Han D, Sun M, Feng J. Long non-coding RNA H19 induces cerebral ischemia reperfusion injury via activation of autophagy. *Aging Dis*. 2017;8:71-84.
26. Nielsen S, Nagelhus EA, Amiry-Moghaddam M, Bourque C, Agre P, Ottersen OP. Specialized membrane domains for water transport in glial cells: high-resolution immunogold cytochemistry of aquaporin-4 in rat brain. *J Neurosci*. 1997;17:171-180.
27. Li Y, Xu QQ, Shan CS, Shi YH, Wang Y, Zheng GQ. Combined use of emodin and ginsenoside Rb1 exerts synergistic neuroprotection in cerebral ischemia/reperfusion rats. *Front Pharmacol*. 2018;9:943.
28. Papadopoulos MC, Verkman AS. Aquaporin-4 and brain edema. *Pediatr Nephrol*. 2007;22:778-784.
29. Thomson DW, Dinger ME. Endogenous microRNA sponges: evidence and controversy. *Nat Rev Genet*. 2016;17:272-283.
30. Zhao L, Sun H, Kong H, Chen Z, Chen B, Zhou M. The Lncrna-TUG1/EZH2 axis promotes pancreatic cancer cell proliferation, migration and EMT phenotype formation through sponging Mir-382. *Cell Physiol Biochem*. 2017;42:2145-2158.
31. Lu Y, Tang L, Zhang Z, et al. Long noncoding RNA TUG1/miR-29c axis affects cell proliferation, invasion, and migration in human pancreatic cancer. *Dis Markers*. 2018;2018:6857042.

## SUPPORTING INFORMATION

Additional supporting information may be found online in the Supporting Information section.

**How to cite this article:** Shan W, Chen W, Zhao X, et al. Long noncoding RNA TUG1 contributes to cerebral ischaemia/reperfusion injury by sponging mir-145 to up-regulate AQP4 expression. *J Cell Mol Med*. 2020;24:250–259. <https://doi.org/10.1111/jcmm.14712>